



# Lightweight and Customized Design via Conformal Parametric Lattice Driven by Stress Fields

Fuyuan Liu, Min Chen<sup>(✉)</sup>, Lizhe Wang, Zhouyi Xiang, and Songhua Huang

School of Advanced Technology, Xi'an Jiaotong-Liverpool University, Suzhou 215000, Jiangsu,  
China

min.chen@xjtlu.edu.cn

**Abstract.** Additive manufacturing has opened up new opportunities for material-based design and optimization, with lattice materials being a key area of interest. Lattice materials can exhibit superb physical properties, such as high thermal conductivity and excellent energy absorption, and be designed to meet specific design objectives. However, optimizing the use of these materials requires considering geometric constraints and loading conditions. This research explores stress-driven multi-agent system (MAS) to achieve high-performance lattice infilling. The von Mises stress and principal stress are investigated as the infilling environments as they are typical failure evaluation criteria. The feasibility of these approaches is demonstrated through a case study of sport helmet design, where MAS is used to generate conformal lattice structures that meet functional and fabrication requirements. The density distribution and arrangement direction of lattice units are effectively controlled in physical fields. The results demonstrate that both von Mises stress field and principal stress field-driven methods can improve the stiffness of helmets compared to the method that only considers geometrical conformity under the same mass. The paper concludes that stress-driven lattice infilling has the potential to revolutionize material-based design and optimization in additive manufacturing.

**Keywords:** Conformal design · Lattice material-based design · Stress-field driven agent system · Design for additive manufacturing

## 1 Introduction

Material development is crucial to optimize product performance, especially for lightweight and customization [1–3]. Additive manufacturing has opened up new opportunities for material-based design and optimization [4]. With designing the morphology of lattice units, lattice material can exhibit superb physical properties that serve different design objectives, such as negative Poisson's ratio, high thermal conductivity, good stiffness, and excellent energy absorption [5]. However, maximizing the utilization of lattice materials under geometric constraints and work conditions can be a challenge.

Loading impact and geometric restrictions are two essential factors that affect the mechanical performance of lattice structures [6]. To address loading impact, two approaches can be taken for lattice infilling: changing the relative density or population orientation. For instance, Wang et al. varied the relative density of cells to resist loading impacts [7]. Stephen et al. constructed principal stress trajectories to infill lattice material graded spatially based on lattice cell orientation [8]. When dealing with geometric restrictions, spatial tessellation is often used to discretize design domains, such as sphere packing and meshing methods [9]. Although many schemes for conformal lightweight design have been proposed, they have yet to be implemented in product design effectively. Moreover, previous studies often overlook the limitations of additive manufacturing. The mechanical performance of lattice structures is greatly influenced by the minimizing feature size, and accurate porosity control is necessary for lattice infilling.

To overcome these challenges, a multi-agent system (MAS) could be a promising solution for high-performance lattice infilling. The high adaptability of generative complexity makes it possible for MAS to generate conformal, functional lattice structures [10–12]. As an integration of numerous intelligent entities, MAS can sense different parameters and perform designated actions in physical fields [13]. For lattice infilling, the von Mises stress field and principal stress field can be regarded as perceived environments for regulating relative density and population orientation, respectively. The pore size of lattice material may be effectively controlled by regulating the movement of agents.

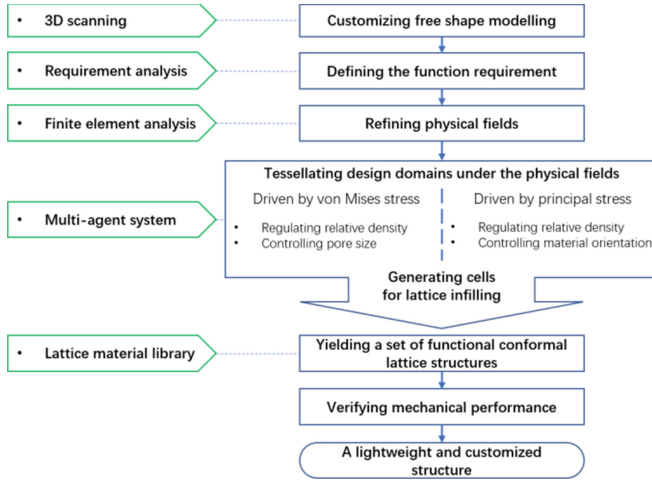
This paper illustrates a case study of sport helmet design in order to explore various lattice infilling methods based on stress-driven MAS. The MAS tessellates design domains into numerous cells to infill the lattice, achieving a conformal lattice structure that satisfies the functional requirements. Agents tessellate design domains under a scalar field by von Mises stress and a vector field by principal stress, respectively. The sport helmets are reformed using customized lattice material, and the feasibility of design methods is demonstrated by compressive testing to improve stiffness. The density distribution and arrangement direction of the lattice units are effectively controlled in physical fields.

## 2 Design Methodology

This work illustrates stress-field-driven lattice infilling methods using sport helmets as examples, since porous lattice structures not only meet customized functions in practical scenarios but also guarantee breathability. This method may improve the wearing experience of users. Additionally, AM accelerates the progress of customized design and fabrication [14]. An integrated approach is proposed here to address material-driven reforming design, as shown in Fig. 1.

### 2.1 Tailoring Free Shape Modelling and Defining the Functional Requirement

For custom-fit sport helmets, the first requirement is to ensure a conformable interaction when users wear helmets. The second requirement is to thicken an inner shell structure



**Fig. 1.** Design framework

in a parametric manner. The method relies on 3D scanning to customize helmet lines to best fit each user's head, avoiding the limitations of standard helmets' sizes and fitting.

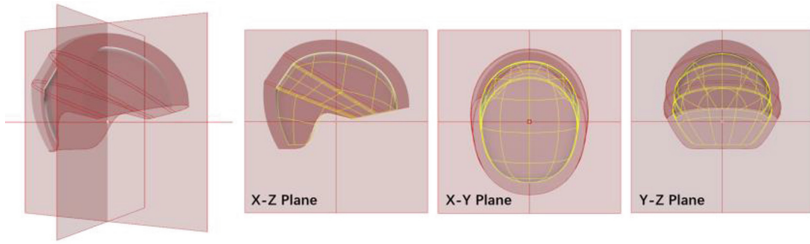


**Fig. 2.** Custom-fit helmet shell

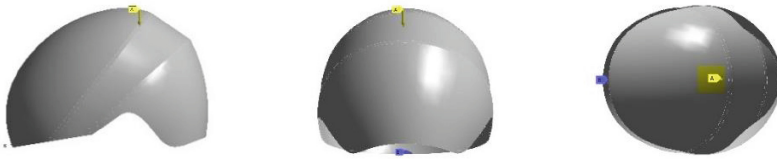
A digital head model is taken as a design reference [16], as shown in Fig. 2. The morphology of the inner layer is consistent with the contour of the head model. The inner shell is scaled outward for a thickened shell. Three parameters are defined to control the size of the outer layers. The mass center of the sport helmet is regarded as the scale center, and the outer layer is scaled based on X-Y, Y-Z, X-Z plane, as shown in Fig. 3. This method enables the design of customized helmets without uncomfortable pressure points and adapts to individual differences.

The functional requirements of the sport helmet are defined according to its application scenario. Structure stiffness is regarded as the optimization target. It is assumed that the load condition of the sports helmet is based on a standard compressive test. The inner layer is numerically analyzed as it directly interacts with the head model. The analysis result is used to refine both von Mises stress data and principal stress data.

As illustrated in Fig. 4, a 1mm displacement is imposed on the inner shell at the yellow label, and blue labels are set as fixed supports. Owing to the size limitation of available 3D printers and testing devices in our lab, the helmet samples are fabricated



**Fig. 3.** Scaling shell structure



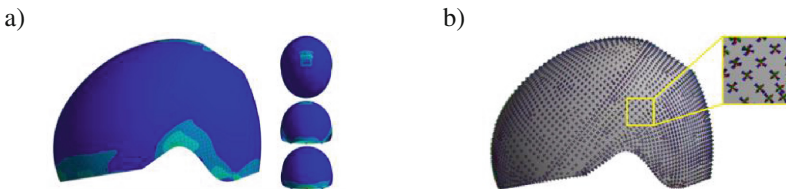
**Fig. 4.** Load and boundary condition for sport helmets

with scaled dimensions. The small displacement ensures the shell structure is in the elastic deformation. FormLab3 white resin is selected as the fabricated material. Its mechanical properties are shown in Table 1.

**Table 1.** Material properties

Density	Young’s modulus	Poisson’s ratio	Yield strength
1100kg/m <sup>3</sup>	251.4MPa	0.23	38.303 MPa

Static structural analysis is executed in ANSYS workbench. Von Mises stress data and principal stress data at each node are exported, as seen in Fig. 5. Both types of data are regarded as the simulated environment for the agent system in next stage.



**Fig. 5.** The results of finite element analysis **a** von Mises stress data **b** Principal stress data

## 2.2 Field-Driven Agent System

Multi-agent systems driven by stress field divide design domains into cells for infilling lattice, achieving a desired conformal lattice structure satisfying function requirements. In material mechanics, there are two typical stress types, von Mises stress and Principal Stress, adapting to different failure mechanisms. The former considers shear stress failure based on the Distortion Energy theory, while the latter adapts to normal stress failure according to the Maximum Normal stress theory. In this paper, the field-driven method based on both types of stresses is discussed.

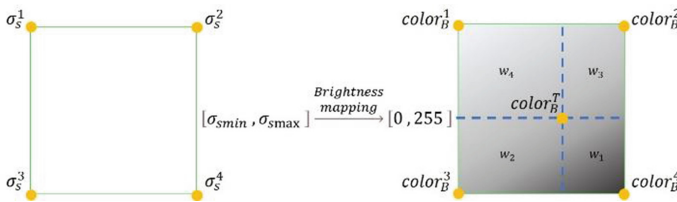
### 2.2.1 Von Mises Field Driven Conformal Design

Von Mises stress is an equivalent stress based on shear strain energy, which can reflect stress intensity suffered by given components, as follows:

$$\sigma_s = \sqrt{\frac{(\sigma_1 - \sigma_2)^2 + (\sigma_2 - \sigma_3)^2 + (\sigma_3 - \sigma_1)^2}{2}} \quad (1)$$

where,  $\sigma_1$ ,  $\sigma_2$ ,  $\sigma_3$  donate the first, second and third principal stress, respectively.  $\sigma_s$  means von Mises stress.

In this strategy, the notion of circle packing is introduced for conformally tessellating the shell structure. Each agent is regarded as a sphere and then disturbs the shell structure without overlapping while the size of spheres decreases as the intensity of von Mises stress increases. The sphere's center is used to construct lattice frames. The image packing algorithm developed by Daniel Pike is employed for regulating the nodes density of lattice, which is realized by Kangaroo, a plugin in Grasshopper™ in the Rhinoceros software package® (Robert McNeel & Associates, Seattle, USA). Here, it establishes a mapping relationship between brightness and von Mises stress intensity, as seen in Fig. 6.



**Fig. 6.** Mapping von Mises stress to Color

Brightness decreases as the intensity of von Mises stress increases. And bilinear interpolation is used to evaluate the  $color_B^T$  by four known color values  $color_B^1$ ,  $color_B^2$ ,  $color_B^3$ , and  $color_B^4$ .

$$color_B^T = w_1 \times color_B^1 + w_2 \times color_B^2 + w_3 \times color_B^3 + w_4 \times color_B^4 \quad (2)$$

$$w_i = \frac{Area_{w_i}}{Area_{total}} \quad i = 1, 2, 3, 4 \quad (3)$$

In addition, the minimum size of the sphere can be regulated for guaranteeing successful manufacturing.

The agents by von Mises stress are following the below behavior principles:

- Behavior 1: Regulating sphere size based on the intensity of a brightness field
- Behavior 2: Separating the agent when the sphere collides with others
- Behavior 3: Only moving on the shell structure
- Behavior 4: Controlling the minimum sphere size for manufacturing restrictions

The specific design procedure can refer to [15]. Finally, all the nodes are used to generate Voronoi or Delaunay wireframes, as shown in Fig. 7.

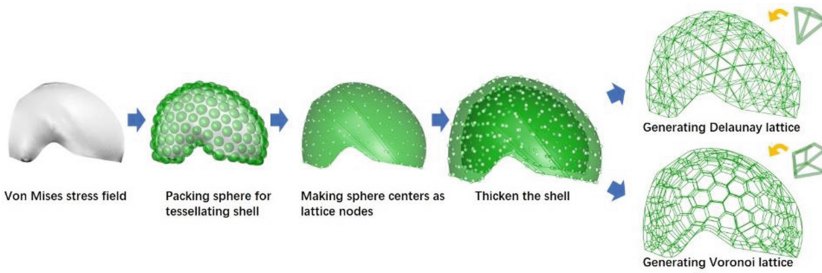


Fig. 7. Sphere packing driven by von Mises stress field

## 2.2.2 Principal Stress Driven Conformal Design

Principal stress is a vector, which can reflect the load transfer mechanism. Brandmaier et al. introduced the effect of the principal stress direction: when the orientation of bars is along principal stress directions in the frame, each bar can suffer the minimum shear stress so as for high stiffness structure [16]. The distribution density of principal stress trajectories reflects the stress intensity and the direction of principal stress represents the effect direction of principal stress. The trajectories guide the generation of truss-based structure.

By finite analysis method, three principal vectors at each node are solved as follows:

$$\begin{bmatrix} \sigma_x - \lambda_1 & \tau_{yx} & \tau_{zy} \\ \tau_{xy} & \sigma_y - \lambda_2 & \tau_{zy} \\ \tau_{xz} & \tau_{yz} & \sigma_z - \lambda_3 \end{bmatrix} \times v_j^{principal} = 0 \times v_j^{principal} \neq 0 \quad j = 1, 2, 3 \quad (4)$$

The  $\sigma$  and  $\tau$  are the normal stress and shear stress at each node, the eigenvector in three directions is donated as  $v_j^{principal}$ .

The principal stress trajectory starts from a seed point  $P_{seed}$  on the domain, the seed point move within the stress field until the point is out of the domain. In each moving, the point will find the nearest FEA node then move along with the principal stress direction that approximates to the pervious moving direction, as below:

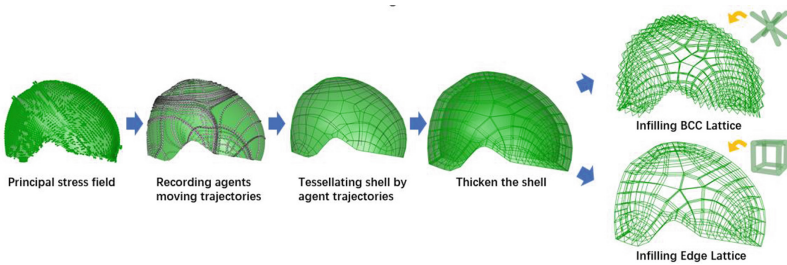
$$P_{i+1} = P_i + \Delta \cdot v_j^{principal} \quad (5)$$

$P_i$  is current position of the agent,  $\Delta$  is a constant, denoted to a moving step.  $v_j^{principal}$  is the principal vector of the node nearest to the  $P_i$ .

The agent by principal stress field is following:

- Behavior 1: Moving along the principal stress vector from the closest node
- Behavior 2: Recording the moving trajectories of each agent
- Behavior 3: Tessellating the shell guiding by each agent trajectories

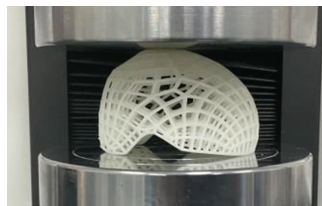
Here, it uses Quad Remesh, a Grasshopper component, to divide the shell of sports helmets into quadrilateral panels under the guidance of principal stress trajectories. Finally, each panel is transformed into an infilling cell by Pufferfish, an open-source plugin of Grasshopper™, as illustrated in Fig. 8.



**Fig. 8.** Principal stress driven lattice infilling

### 3 Physical Experiment and Discussion

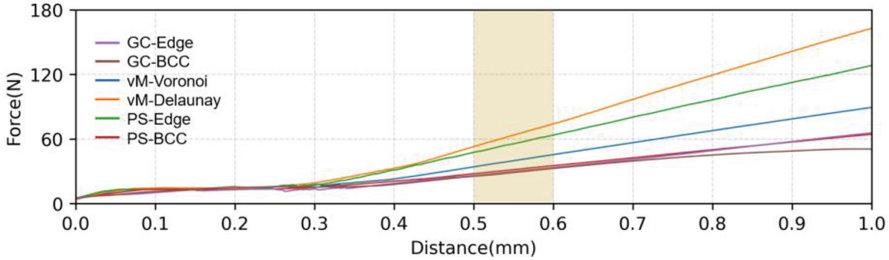
The abovementioned wireframes are transferred into solid model by Dendro, an open-source plugin for Grasshopper™. All optimized helmet samples are fabricated by Stereo lithography Appearance (SLA) on FormLab3 and conducted compressive tests on SanSiZongHeng universal testing machines to verify the advantages of the two methods.



**Fig. 9.** Compressive testing

The experiment aims to demonstrate whether conformal gradient lattice infilling can improve the stiffness of sports helmets, as shown in Fig. 9. The lattice sport helmet only considering geometric conformal infilling is regarded as a comparative group. A just

geometric conformal helmet is generated directly by Quad Remesh component without the guidance of any curves. The displacement of 1 mm/min is imposed on all the samples and the Force-Distance curves are shown in Fig. 10.



**Fig. 10.** The force-displacement curves of all samples

Compressive tests were performed by the proposed method and the results were illustrated as shown in Table 2. The weight of all the samples was controlled at 8.00 g. A Force-Displacement curve is obtained by three points bending experiments. According to the results of experiments, the linear stiffnesses of all samples are calculated with following Eq. (6):

$$k = \frac{\Delta F}{\Delta \delta} \quad (6)$$

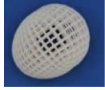
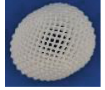


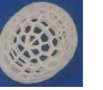

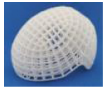

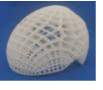
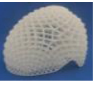
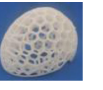
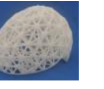
where,  $k$  is denoted by linear stiffness.  $F$  is a force suffered by samples, and  $\delta$  is a displacement produced by the force.  $\Delta F/\Delta \delta$  is the slope of the force-displacement curve when the linear elastic deformation happens. The displacements at 0.5–0.6 mm and their responding forces are used for calculating the linear stiffness of samples, as illustrated in Table 2. Each structure produced five samples for comparison.

By comparison, it was found that samples vM-Voronoi, vM-Delaunay, and PS-Edge increase linear stiffness by over 0.6 times over geometric conformal lattice structures. This demonstrates that gradient lattice structure benefits stiffness optimization. Theoretically, the principal stress-driven method can present higher mechanical performance than the von Mises stress-driven method. Because the von Mises-driven method prefers to solve local stress concentration and achieves a gradient distribution of lattice material, whereas principal stress trajectories take the load transfer mechanism into account and regulate both lattice density and orientation. However, the results show that the von Mises stress-driven method has the highest linear stiffness among all samples. The main reason for this is that it adds an exponential factor to reinforce the effect range of the von Mises stress field, and then make the density distribution of lattice material reasonable, as referred to (15).

Another important consideration when infilling the lattice material is its anisotropy, especially when using the principal stress-driven method. In Group 1 and Group 2, two types of lattice structures were used: PS-Edge and GC-Edge, which are edge-cubic lattices, and PS-BCC and GC-BCC, which are body center cubic lattices. The edge-cubic lattice is 90° orthotropic, which allows stress transfer direction to align with the material's maximum Young's modulus, resulting in high stiffness. However, the body



**Table 2.** Samples by additive manufacturing

Method	Group 1: Geometric conformal design		Group 2: Principal stress driven conformal design		Group 3: von mises stress driven conformal design	
Top view						
Side view						
ID	GC-Edge	GC-BCC	PS-Edge	PS-BCC	vM-Voronoi	vM-Delaunay
Mass	8.06	8.71	8.28	8.27	7.70	8.24
Linear stiffness	75.33	69.60	167.06	72.68	111.33	228.43

center cubic lattice has a  $45^\circ$  orthotropic, meaning that the lattice mainly suffers from bending forces, resulting in low linear stiffness.

## 4 Conclusion

This research presents two stress-driven MAS that release the full potential of lattice material and optimize the mechanical performance of sports helmets. By dividing the helmets into cells and infilling them with lattice material in a conformal manner under von Mises stress and principal stress, the density and orientation of the lattice material can be regulated to achieve functional, lightweight, and customized designs.

Compressive testing verified that the stress-driven methods produced products with superior performance compared to designs that only considered geometric conformal design. Additionally, the methods enable products with both high performance and aesthetically pleasing natural-like structures.

The MAS driven by the von Mises stress field allows for gradient material population, while also considering the minimum size features of the lattice material for successful fabrication. The MAS driven by the principal stress field can effectively regulate the populating orientation of the lattice material for improving stiffness. These design concepts can be further integrated with a lattice library to meet diverse functional requirements and personalized user preferences.

The proposed methods have the potential for broad industrial applications, such as in Unmanned Aerial Vehicles (UAVs) and automobiles. The methods can be integrated into automatic and iterative design progress, such as genetic algorithms, to yield diverse design outputs with robust mechanical performance.

**Acknowledgement.** This work was supported by the Research Development Fund of Xi'an Jiaotong-Liverpool University [RDF-17-02-44, RDF-SP-122], Industry Research & Development Projects [RP0028, RP0029] and XJTU AI University Research Centre.

## References

1. Seharing, A., Azman, A.H., Abdullah, S.: A review on integration of lightweight gradient lattice structures in additive manufacturing parts. *Adv. Mech. Eng.* **12**(6), 1687814020916951 (2020)
2. Pan, C., Han, Y., Lu, J.: Design and optimization of lattice structures: A review. *Appl. Sci.* **10**(18), 1–36 (2020)
3. Tamburrino, F., Graziosi, S., Bordegoni, M.: The design process of additively manufactured mesoscale lattice structures: A review. *J. Comput. Inf. Sci. Eng.* **18**(4), 1–16 (2018)
4. Sharma, D., Babel, P.V.: Design for additively manufactured structure: an assessment. *Int J Trend Sci Res Dev.* **3**(3), 85–89 (2019)
5. Jia, Z., Liu, F., Jiang, X., Wang, L.: Engineering lattice metamaterials for extreme property, programmability, and multifunctionality. *J Appl Phys.* **127**(15), (2020)
6. Nguyen, J., Park, S.I., Rosen, D.W., Folgar, L., Williams, J.: Conformal lattice structure design and fabrication. In: 2012 International solid freeform fabrication symposium. University of Texas at Austin, pp. 138–161. (2012)
7. Wang, Y., Xu, H., Pasini, D.: Multiscale isogeometric topology optimization for lattice materials. *Comput. Methods Appl. Mech. Eng [Internet].* **316**, 568–585 (2017). Available from <https://doi.org/10.1016/j.cma.2016.08.015>
8. Daynes, S., Feih, S., Lu, W.F., Wei, J.: Optimisation of functionally graded lattice structures using isostatic lines. *Mater Des [Internet].* **127**, 215–223 (2017). Available from <https://linkin.gub.elsevier.com/retrieve/pii/S0264127517304392>
9. van Sosin, B., Rodin, D., Sliusarenko, H., Bartoň, M., Elber, G.: The construction of conforming-to-shape truss lattice structures via 3D sphere packing. *CAD Comput Aided Des.* **1**(132), 102962 (2021)
10. Bao, D.W., Yan, X., Xie, Y.M.: Encoding topological optimisation logical structure rules into multi-agent system for architectural design and robotic fabrication. *Int J Archit Comput.* **0**(0), 147807712210822 (2022)
11. Macal, C.M., North, M.J.: Agent-based modelling and simulation. In: *Proc 2009 Winter Simul Conference*, pp. 86–98. (2009)
12. Bao, D.W., Yan, X., Snooks, R., Xie, Y.: Swarms: Multi-agent and evolutionary computational design based on the principles of structural performance. In: *Proc 26th Int Conf Assoc Comput Archit Des Res Asia, CAADRIA 2021*, vol. 1, pp. 241–250. (2021)
13. Dorri, A., Kanhere, S.S., Jurdak, R.: Multi-agent systems: A survey. *IEEE Access* **6**, 28573–28593 (2018)
14. Jing, S.K., Song, G.H., Liu, J.H., Zhou, J.T., Zhang, H.: A review of product design for additive manufacturing. *Appl. Mech. Mater.* **635–637**, 97–100 (2014)
15. Liu, F., Chen, M., Wang, L., Luo, T., Chen, G.: Stress-field driven conformal lattice design using circle packing algorithm. *Heliyon [Internet].* **9**(3), e14448 (2023). Available from: <https://doi.org/10.1016/j.heliyon.2023.e14448>
16. Brandmaier, H.: Optimum filament orientation criteria. *J. Compos. Mater.* **4**(July), 422–425 (1970)

**Open Access** This chapter is licensed under the terms of the Creative Commons Attribution 4.0 International License (<http://creativecommons.org/licenses/by/4.0/>), which permits use, sharing, adaptation, distribution and reproduction in any medium or format, as long as you give appropriate credit to the original author(s) and the source, provide a link to the Creative Commons license and indicate if changes were made.

The images or other third party material in this chapter are included in the chapter's Creative Commons license, unless indicated otherwise in a credit line to the material. If material is not included in the chapter's Creative Commons license and your intended use is not permitted by statutory regulation or exceeds the permitted use, you will need to obtain permission directly from the copyright holder.

